Wireless Pers Commun
DOI 10.1007/s11277-010-9930-x

Carrier Frequency Offset in VSF-OFCDM Systems with Subcarrier Grouping: Analysis, Estimation and Correction

Lamiaa Khalid · Alagan Anpalagan

Abstract We investigate the effect of carrier frequency offset (CFO) on the performance of downlink variable spreading factor (VSF) orthogonal frequency and code division multiple access (OFCDM) systems when subcarrier grouping is used. An analytic expression of the signal to interference and noise ratio (SINR) is derived for the VSF-OFCDM with CFO for the case of maximal ratio combining (MRC) and equal gain combining (EGC) receivers. Numerical results show that, when the total spreading factor is fixed, a system with higher frequency domain spreading factor is more sensitive to CFO than that with lower frequency domain spreading factor. Also, for high E_b/N_o, EGC has better bit error rate performance than MRC due to the greater interference amplification present in MRC which compounds the effect of the loss of orthogonality. Due to the adverse impact of the CFO on VSF-OFCDM systems, we propose a correction scheme based on the maximum likelihood principle. We then use a gradient algorithm to estimate and minimize the effect of CFO in a tracking mode. Our results show that the BER performance in the low SINR environment can be improved significantly with few number of iterations for different spreading factors.

Keywords OFCDM systems · Carrier frequency offset · Subcarrier grouping · Estimation and correction

A part of this article was presented in 2008 IEEE International Conference on Communications in Beijing, China.
This work was in part supported by the Natural Sciences and Engineering Research Council (NSERC) of Canada.

L. Khalid · A. Anpalagan (✉)
Department of Electrical and Computer Engineering, Ryerson University,
Toronto, ON, Canada
e-mail: alagan@ee.ryerson.ca

Published online: 16 February 2010

1 Introduction

Orthogonal frequency and code division multiplexing (OFCDM) system has been proposed for future broadband wireless communications [1]. OFCDM uses data spreading in both time and frequency domain, where each data stream is segmented into multiple substreams and spread over multiple subcarriers and several OFCDM symbols, exploiting additional frequency and time diversity. The variable spreading factor (VSF) concept for OFCDM was introduced in [2], where the spreading factor (SF) in both the time and frequency domain is varied. The total spreading factor is the product of time domain spreading factor (SF_{time}) and frequency domain spreading factor (SF_{freq}). One of the main characteristics of VSF-OFCDM is that SF_{time} and SF_{freq} can be adaptively controlled according to the propagation conditions, channel load and radio parameters [3].

One of the main drawbacks of multicarrier systems is that they suffer from performance degradation due to carrier frequency offset (CFO). In general, OFDM systems are less sensitive to time offset than single carrier systems [4]. CFO causes a reduction in the desired signal amplitude as well as loss of orthogonality between subcarriers which results in inter-carrier interference (ICI). The impact of frequency offset on multicarrier systems was investigated in [5] and [6] for multicarrier code division multiple access (MC-CDMA) and group-orthogonal MC-CDMA, respectively and, in [7] for both uplink and downlink multicarrier direct sequence code division multiple access (MC-DS-CDMA) systems. Recently, there are some papers in the literature investigating the effect of frequency offset on OFCDM systems. In [8], the BER performance of multiple antenna OFCDM systems with imperfections was studied. In [9], the sensitivity of OFDM-CDMA systems to carrier frequency offset was investigated for zero forcing and minimum mean square error equalizers. However, no subcarrier grouping was considered in their analysis, although the subcarrier grouping strategy has an impact on the different types and amount of interference introduced with frequency offset. Also, the effect of using variable spreading factors on the BER performance of OFCDM systems was not investigated in their work.

In this article, the effect of the frequency offset is first analyzed by investigating the type and the amount of interference caused by CFO in VSF-OFCDM systems with different spreading factors. An analytic expression of the SINR for downlink VSF-OFCDM with frequency offset is derived for the case of maximal ratio combining (MRC) and equal gain combining (EGC) receivers [10]. In our analysis, the standard Gaussian approximation [11] is applied to the interference and noise terms. Due to the adverse impact of frequency offset on VSF-OFCDM systems, a reliable estimation of the frequency offset is then considered as a basic step in the coherent demodulation process. The CFO estimation process can be divided into two fundamental steps which are coarse acquisition and tracking. In this article, we focus on the estimation and correction of the frequency offset in a tracking mode. For orthogonal frequency division multiplexing (OFDM) and MC-CDMA systems, similar algorithms have been proposed in [12] and [13], respectively. In our work, a CFO correction scheme based on maximum likelihood (ML) estimation is proposed for OFCDM systems with different spreading factors using MRC and EGC receivers. Our results show that the proposed method can minimize the normalized frequency offset residual error significantly after only few iterations. This error minimization results in noticeable improvement in the system performance in terms of the BER.

The article is organized as follows: Sect. 2 gives a brief description of the OFCDM transmitter and receiver. In Sect. 3, the BER of VSF-OFCDM is derived in the presence of CFO for MRC and EGC receivers and then numerical results are presented. In Sect. 4, the likelihood function for VSF-OFCDM system with CFO is derived and then the gradient method is used

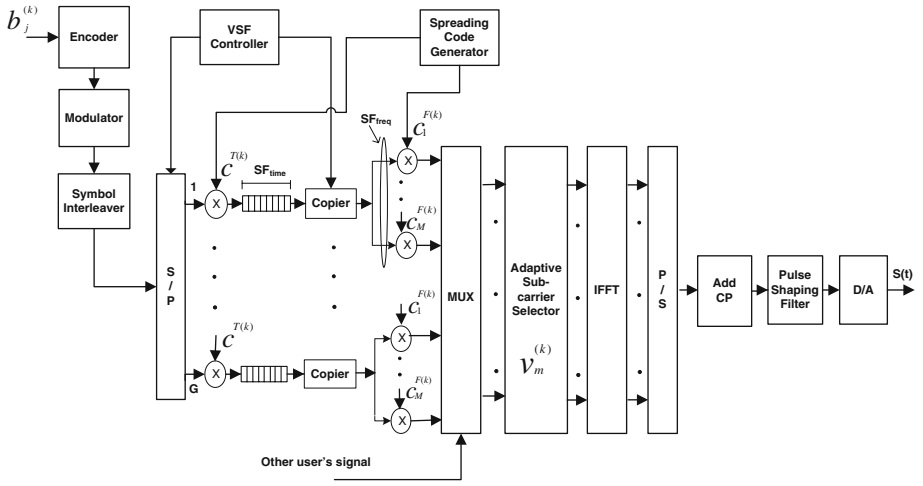

Fig. 1 VSF-OFCDM transmitter

to correct the CFO. Numerical results are presented there as well. Finally, conclusions are given in Sect. 5.

2 VSF-OFCDM System Model

2.1 VSF-OFCDM Transmitter

In this work, an OFCDM system with K simultaneous users is considered. The total spectrum is divided into G groups; each group has M non-contiguous subcarriers that are equally spaced throughout the spectrum. A block diagram of the VSF-OFCDM transmitter is shown in Fig. 1. Each data symbol is spread in the time domain with N chips, where N is equal to SF_{time}, and in the frequency domain with SF_{freq} chips which is equal to the M subcarriers in each group g. Therefore, totally $\mathrm{SF}(= \mathrm{SF}_{time} \times \mathrm{SF}_{freq})$ spread chips per data symbol are involved in the 2-D spreading. The 2-D code assigned to the kth user is denoted as $[c^{T(k)}, c^{F(k)}]$, where $c^{T(k)}$ is the time domain spreading code of length N and $c^{F(k)}$ is the frequency domain spreading sequence of length M.

At the transmitter, the bit stream of the kth user during the jth signal element, b_j^k, is first encoded and then mapped into symbols by the data modulator. A symbol interleaver [14] is employed to separate successive symbols to non adjacent subcarriers to randomize the deep faded symbols due to frequency selective fading. Interleaved data symbols are then serial-to-parallel (S/P) converted into G substreams. After S/P conversion, 2-D spreading is carried out, where each data symbol is first spread into chips in time domain with the spreading code $c^{T(k)}$ and then the time-domain spread signal is duplicated into M copies and each copy is multiplied by a chip of the frequency domain spreading code $c^{F(k)}$. The spread signals from different users are added together by the multiplexer. An adaptive subcarrier selector block is then used that allows subcarriers to be selected adaptively based on the channel conditions. The parameters used by this block are determined by the adaptive subcarrier allocation algorithm proposed in [15]. The resultant signals are then up-converted into the selected subcarriers using an L point inverse fast Fourier transform (IFFT) [16], where L is a power

of 2. After IFFT, the OFCDM symbol is obtained. Then, a guard interval is inserted between OFCDM symbols to prevent intersymbol interference (ISI). Finally, the complete OFCDM symbol passes through a pulse shaping filter, which gives rise to the baseband transmitted signal.

Therefore, assuming BPSK modulation, the transmitted signal for the kth user can be written as:

$$s^{(k)}(t) = \sqrt{2P} \sum_{j} \sum_{g=1}^{G} b_{j,g}^{(k)} \sum_{l=1}^{M} v_{j,l,g}^{(k)} c_{j,l}^{F(k)} \cos(\omega_{l,g} t) \sum_{n=1}^{N} c_{j,l,n}^{T(k)} p(t - (jN + n)T_c), \quad (1)$$

where P is the transmitted power on one subcarrier. The bit stream of the kth user on the gth group during the jth signal element, $b_{j,g}^{(k)}$, is equal to ± 1. $c_{j,l,n}^{T(k)}$ is the nth chip in the time domain spreading code on the lth subcarrier and $c_{j,l}^{F(k)}$ is the lth chip in the frequency domain spreading sequence of length M during the jth transmitted symbol. The parameter $v_{j,l,g}^{(k)} = 1$, if the lth subcarrier of the gth group is assigned to the kth user by the adaptive subcarrier allocation algorithm. If the lth subcarrier of the gth group is not assigned to user k, user k does not transmit data over this subcarrier and $v_{j,l,g}^{(k)} = 0$. $p(t)$ is the waveform of the pulse shaping filter and it is defined on the interval $[0, T_c]$, where T_c is the chip duration of the time domain spreading code, and it can be written as:

$$p(t - (jN + n)T_c) = \begin{cases} 1, & (jN + n)T_c \le t \le (jN + n + 1)T_c; \\ 0, & \text{elsewhere.} \end{cases}$$

Here, $\omega_{l,g}$ is the frequency of the lth subcarrier of the gth group and it can be written as

$$\omega_{l,g} = \omega_c + \frac{2\pi(g + (l-1)G)}{T_c},$$

where ω_c is the carrier frequency and $1/T_c$ is the frequency spacing between two adjacent subcarriers. The impulse response of the channel for the kth user and the lth subcarrier of the gth group is described as [17]:

$$h_{l,g}^{(k)}(t, j) = \alpha_{l,g}^{(k)}(t, j) e^{i\left(\phi_{l,g}^{(k)}\right)}, \quad (2)$$

where $\alpha_{l,g}^{(k)}$ are independent identically distributed (i.i.d.) Rayleigh random variables for the kth user on the lth subcarrier of the gth group during the jth transmitted OFCDM symbol. The phase, $\phi_{l,g}^{(k)}$, is a uniformly distributed random variable over the interval $[0, 2\pi)$, which is independent for each symbol, subcarrier and user. Furthermore, the channel fading and phase shift variables are considered to be constant over a chip duration T_c. The received signal is a sum of all the K users' signals transmitted during the jth signal element. These signals are all corrupted by independent fading conditions, as well as Additive White Gaussian Noise (AWGN). Consequently, the received signal is expressed as

$$r(t) = \sum_{k=1}^{K} s^{(k)}(t) * h^{(k)}(t) + n(t), \quad (3)$$

where $h^{(k)}(t)$ represents the total impulse response across all subcarriers for user k, $n(t)$ is the AWGN with zero mean and double-sided power spectral density $N_0/2$ and $(*)$ denotes the convolution process.

Various adaptive subcarrier allocation algorithms were proposed for MC-CDMA and MC-DS-CDMA systems [18]. Many of these algorithms outperform the corresponding

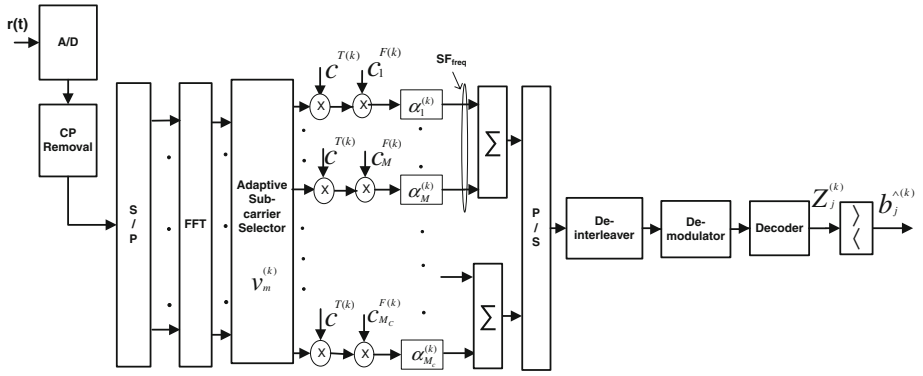

Fig. 2 VSF-OFCDM receiver for user k

non-adaptive systems in terms of the BER performance. An adaptive subcarrier allocation algorithm was proposed to maximize the overall BER performance under different spreading factors in [15] and we use this algorithm in our work. In this algorithm, the total spectrum is separated into small groups of non-contiguous subcarriers to maximize frequency diversity gains and minimize MAI. The users are assigned to subcarriers based on the instantaneous SINR characteristics of each subcarrier such that the average SINR of the system is maximized while minimizing the interference caused to other users simultaneously.

2.2 VSF-OFCDM Receiver

The VSF-OFCDM receiver block diagram is shown in Fig. 2. The received signal is given by (4) where K_g is the total number of users in group g.

$$r(t) = \sqrt{2P} \sum_{j} \sum_{g=1}^{G} \sum_{k=1}^{K_g} b_{j,g}^{(k)} \sum_{l=1}^{M} \alpha_{l,g}^{(k)} c_{j,l}^{F(k)} \cos\left(\omega_{l,g} t + \phi_{l,g}^{(k)}\right) \times \sum_{n=1}^{N} c_{j,l,n}^{T(k)} p(t - (jN + n)T_c) + n(t), \tag{4}$$

Assuming that the guard interval is larger than the maximum path delay spread, there is no ISI in the received signals. Without loss of generality, we aim to recover the data transmitted to user 1 in group 1. We first convert the received signal into parallel format using the serial-to-parallel converter and then multiply by the subcarrier allocation coefficients for user 1, $v_{j,m,1}^{(1)}$. This ensures that only the allocated subcarriers are detected at the receiver. After the fast Fourier transform (FFT) block, the received signal is correlated with the synchronized time and frequency domain spreading sequences for user 1, $[c^{T(1)}, c^{F(1)}]$. The signal on the mth subcarrier is first correlated with the synchronized time domain spreading sequence for user 1, $c^{T(1)}$. The output of each time domain correlator is then multiplied by a chip from the frequency domain spreading code of user 1, $c^{F(1)}$, to remove the frequency domain spreading. The output is then combined at the frequency domain despreader and multiplied by the path weight for the corresponding subcarrier. The receiver uses the MRC algorithm to maximize the SINR at the output of the correlator. In this combining algorithm, the weight given to the mth subcarrier in group 1 is equivalent to the fading gain on this subcarrier,

$\alpha_{m,1}^{(1)}$. EGC is identical to MRC except that a gain of unity is applied to each subcarrier. After parallel-to-serial (P/S) conversion, the output is demodulated, decoded and sampled to yield the decision variable for the kth user at the jth transmitted signal. The decision variable for user 1 in group 1 is given by (5) where $\hat{\phi}_{m,1}^{(1)}$ denotes the estimated phase of the mth subcarrier of group 1 during the jth transmitted bit to user 1.

$$z_{j,1}^{(1)} = \sum_{m=1}^{M} \sum_{n=1}^{N} \frac{1}{T_c} \int_{(jN+n)T_c}^{(jN+n+1)T_c} \alpha_{m,1}^{(1)} c_{j,m}^{F(1)} c_{j,m,n}^{T(1)} r(t) \cos\left(\omega_{m,1} t + \hat{\phi}_{m,1}^{(1)}\right) dt, \tag{5}$$

3 Effects of CFO

The effect of the frequency offset is analyzed by investigating the type and the amount of interference caused by CFO in VSF-OFCDM systems with different spreading factors when subcarrier grouping is used.

3.1 Bit Error Rate Analysis

In this section, an analytic expression of the SINR (and then BER) for downlink VSF-OFCDM with frequency offset is derived for the case of MRC and EGC receivers. The maximum Doppler spread is assumed to be smaller with respect to the subcarrier spacing; therefore, we consider the CFO caused by this spread as a common phenomenon in all the subcarriers [5]. We also assume that each subcarrier experiences flat fading.

Taking into account the frequency offset $f_d^{(k)}$, the impulse response of the channel for the kth user and the lth subcarrier of the gth group during the jth transmitted bit can be described as [17]:

$$h_{l,g}^{(k)}(t, j) = \alpha_{l,g}^{(k)}(t, j) e^{i\left(2\pi f_d^{(k)} t + \phi_{l,g}^{(k)}\right)}. \tag{6}$$

Therefore, the received signal with CFO, can be written as:

$$r(t) = \sqrt{2P} \sum_{j} \sum_{g=1}^{G} \sum_{k=1}^{K_g} b_{j,g}^{(k)} \sum_{l=1}^{M} \alpha_{l,g}^{(k)} c_{j,l}^{F(k)} \cos\left(\omega_{l,g} t + \phi_{l,g}^{(k)} + \omega_d^{(k)} t\right) \times \sum_{n=1}^{N} c_{j,l,n}^{T(k)} p(t - (jN + n)T_c) + n(t), \tag{7}$$

If we consider MRC in our analysis, the decision variable for user 1 in group 1 is given by (5). For simplicity of further calculations, the decision variable can be expressed as

$$z_{j,1}^{(1)} = S + \eta + \text{MAI} + \text{ICI}_1 + \text{ICI}_2 + \text{ICI}_g, \tag{8}$$

where S is the desired signal term; η is the noise term; MAI represents the multiple access interference imposed by the interfering users in the same group of the desired user from the same subcarriers, where the considered subcarriers are $m = 1, \ldots, M$; ICI_1 is the self-intercarrier interference from the other subcarriers of the same group; ICI_2 is the multiple access intercarrier interference imposed by the interfering users in the same group of the desired user, but associated with the subcarriers different from the considered subcarrier and ICI_g is the intergroup interference which represents the intercarrier interference from subcarriers in

other groups. Without loss of generality, these parameters are considered for user 1 in group 1 at the jth transmitted bit. In the Appendix, the above terms are derived for the case of MRC receiver. In our analysis, we consider downlink transmission; therefore, we can assume that all the users suffer equal fading gain and phase shift on each subcarrier [6], which means that $\alpha_{m,g}^{(k)} = \alpha_{m,g}$, and we can further simplify the derived equations as follows:

$$\sigma_\eta^2 = \frac{NN_0}{4T_c} \sum_{m=1}^{M} (\alpha_{m,1})^2, \tag{9}$$

$$\sigma_{\mathrm{MAI}}^2 = N\frac{P}{4}(K_1 - 1)\frac{\sin^2(\pi f_d T_c)}{(\pi f_d T_c)^2} \sum_{m=1}^{M} (\alpha_{m,1})^4, \tag{10}$$

$$\sigma_{\mathrm{ICI}_1}^2 = N\frac{P}{4\pi^2}\sin^2(\pi f_d T_c) \sum_{m=1}^{M} (\alpha_{m,1})^2 \sum_{\substack{l=1 \\ l\neq m}}^{M} \frac{(\alpha_{l,1})^2}{(f_d T_c + (l-m)G)^2}, \tag{11}$$

$$\sigma_{\mathrm{ICI}_2}^2 = N(K_1 - 1)\frac{P}{4\pi^2}\sin^2(\pi f_d T_c) \sum_{m=1}^{M} (\alpha_{m,1})^2 \sum_{\substack{l=1 \\ l\neq m}}^{M} \frac{(\alpha_{l,1})^2}{(f_d T_c + (l-m)G)^2}, \tag{12}$$

$$\sigma_{\mathrm{ICI}_g}^2 = N\frac{P}{4\pi^2}\sin^2(\pi f_d T_c) \sum_{g=2}^{G} \sum_{m=1}^{M} \sum_{l=1}^{M} \frac{K_g(\alpha_{l,g})^2(\alpha_{m,1})^2}{(f_d T_c + (g-1) + (l-m)G)^2}. \tag{13}$$

In the case of EGC receiver $\alpha_{m,1}^{(1)} = 1$ in (5) and the noise and interference terms are given as follows:

$$\sigma_{\eta_{\mathrm{EGC}}}^2 = \frac{MNN_0}{4T_c}, \tag{14}$$

$$\sigma_{\mathrm{MAI}_{\mathrm{EGC}}}^2 = N\frac{P}{4}(K_1 - 1)\frac{\sin^2(\pi f_d T_c)}{(\pi f_d T_c)^2} \sum_{m=1}^{M} (\alpha_{m,1})^2, \tag{15}$$

$$\sigma_{\mathrm{ICI}_{1_{\mathrm{EGC}}}}^2 = N\frac{P}{4\pi^2}\sin^2(\pi f_d T_c) \sum_{m=1}^{M} \sum_{\substack{l=1 \\ l\neq m}}^{M} \frac{(\alpha_{l,1})^2}{(f_d T_c + (l-m)G)^2}, \tag{16}$$

$$\sigma_{\mathrm{ICI}_{2_{\mathrm{EGC}}}}^2 = N(K_1 - 1)\frac{P}{4\pi^2}\sin^2(\pi f_d T_c) \sum_{m=1}^{M} \sum_{\substack{l=1 \\ l\neq m}}^{M} \frac{(\alpha_{l,1})^2}{(f_d T_c + (l-m)G)^2}, \tag{17}$$

$$\sigma_{\mathrm{ICI}_{g_{\mathrm{EGC}}}}^2 = N\frac{P}{4\pi^2}\sin^2(\pi f_d T_c) \sum_{g=2}^{G} \sum_{m=1}^{M} \sum_{l=1}^{M} \frac{K_g(\alpha_{l,g})^2}{(f_d T_c + (g-1) + (l-m)G)^2}. \tag{18}$$

The SINR of user 1 in group 1 during the jth bit can be expressed as

$$\gamma_{j,1}^{(1)} = \frac{E^2[S]}{\sigma_{\mathrm{MAI}}^2 + \sigma_{\mathrm{ICI}_1}^2 + \sigma_{\mathrm{ICI}_2}^2 + \sigma_{\mathrm{ICI}_g}^2 + \sigma_\eta^2}, \tag{19}$$

where in the case of MRC receiver

$$E^2[S]_{\mathrm{MRC}} = \frac{N^2 P}{2}\frac{\sin^2(\pi f_d T_c)}{(\pi f_d T_c)^2}\left(\sum_{m=1}^{M} \alpha_{m,1}^2\right)^2, \tag{20}$$

and in the case of EGC receiver

$$E^2[S]_{\text{EGC}} = \frac{N^2 P}{2} \frac{\sin^2(\pi f_d T_c)}{(\pi f_d T_c)^2} \left(\sum_{m=1}^{M} \alpha_{m,1} \right)^2 . \tag{21}$$

The probability of error based on the Gaussian assumption for BPSK modulation can be expressed as

$$P_e = \text{Q}\left(\sqrt{2\gamma_{j,1}^{(1)}} \right), \tag{22}$$

where $Q(x) = \frac{1}{2\pi} \int_x^\infty e^{\frac{-x^2}{2}} dx$.

3.2 BER Numerical Results

In this section, we consider a VSF-OFCDM system with 128 subcarriers. We assume that each subcarrier experiences flat fading and that fading is uncorrelated between subcarriers in the same group as a result of the subcarrier grouping strategy used. In our evaluation, the gain on each subcarrier is independent, identically distributed Rayleigh random variable. The update period of the adaptive subcarrier allocation algorithm is selected to be equivalent to the coherence time of the channel to ensure that the channel is constant over the update period [15]. In OFCDM, each data stream is segmented into multiple substreams and spread over multiple subcarriers and several OFCDM symbols as mentioned before. The data rate for each user in each analysis is kept constant by transmitting a number of substreams equal to a multiple of the number of chips in the time domain spreading code N. In this evaluation, $2N$ substreams are simultaneously transmitted for each user.

The different spreading factors can be used to provide different levels of frequency diversity, or to minimize MAI in the event of high channel loads. SF_{time} is equal to the N chips in the time domain spreading code and SF_{freq} is equal to the M subcarriers in each group g. We consider a VSF-OFCDM system having carrier frequency offsets of 0, 10, 20 and 30% of the frequency spacing between adjacent subcarriers [10]. Each of the configurations uses a total spreading factor $\text{SF} = \text{SF}_{time} \times \text{SF}_{freq}$ of 32 to provide a suitable performance comparison. We use a total SF of 2×16 to represent a case with high frequency domain spreading and 16×2 to represent a case with high time domain spreading, respectively. We also use a total SF of 8×4 and 4×8 to represent cases of using moderate levels of time and frequency domain spreading for VSF-OFCDM systems. The effect of CFO on the mean BER performance with different spreading factors is investigated by using Monte-Carlo simulation with 1,000 runs and with the above mentioned parametric values.

Figures 3 and 4 show the BER versus E_b/N_o for 16 users with total SF of 2×16 and 16×2, respectively for the case of MRC and EGC receivers. It can be observed from these figures that, for both MRC and EGC receivers, the degradation in BER caused by CFO is insignificant at very low E_b/N_o. However, as E_b/N_o increases the OFCDM system makes a transition from being noise-limited to being interference-limited, and the degree of degradation increases as well. We can observe from the figures that the MRC receiver outperforms the EGC receiver in the low and average SNR regions. However, for high E_b/N_o, $E_b/N_o > 30$ dB, EGC performs better than MRC due to the greater interference amplification present in MRC which compounds the effect of the loss of orthogonality. It can also be seen from the figures that, for both receivers, the degradation in BER caused by the CFO increases with higher SF_{freq} because of the fact that more subcarriers are present in each group which increases the intercarrier

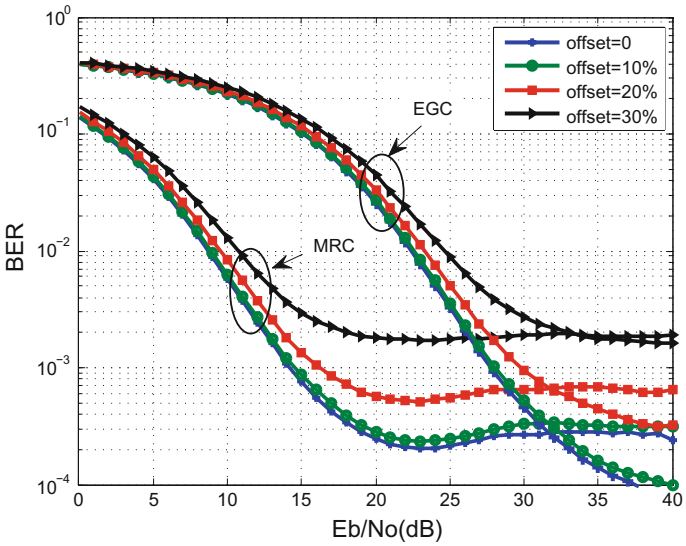

Fig. 3 BER performance comparison of MRC and EGC with SF $= 2 \times 16$ and 16 users at different normalized frequency offsets

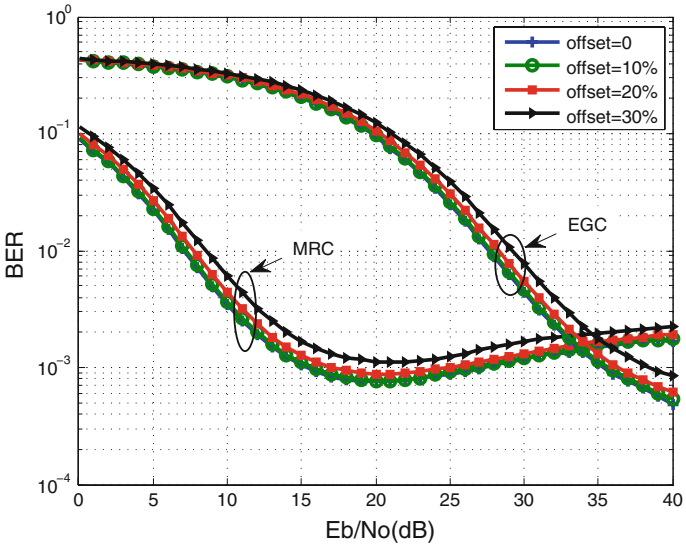

Fig. 4 BER performance comparison of MRC and EGC with SF $= 16 \times 2$ and 16 users at different normalized frequency offsets

interference. From Fig. 4, we can see that for the case of low $\mathrm{SF}_{freq}(\mathrm{SF}_{freq} = 2)$, MAI is the main factor that causes the performance degradation since there are fewer subcarriers in each group which decreases the effect of the intercarrier interference due to frequency offset than the case with higher $\mathrm{SF}_{freq}(\mathrm{SF}_{freq} = 16)$. Although the achieved BER performance associated with MRC and EGC will depend on the SNR as well as the number of users, similar observations can be made on the comparison between MRC and EGC receivers and

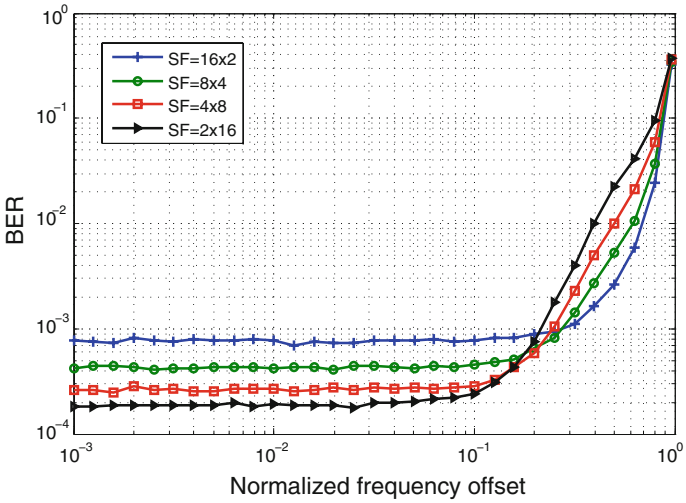

Fig. 5 BER of MRC receiver versus normalized frequency offset at $E_b/N_o = 20$ dB for different SF

the effect of carrier frequency offset on their performance when the number of users are increased from 16 to 32 users.

Figure 5 shows the BER of the MRC receiver versus the normalized frequency offset with respect to the subcarrier spacing for different spreading factors with $E_b/N_o = 20$ dB. From Fig. 5, it can be observed that at high E_b/N_o, higher SF_{freq} performs better than higher SF_{time} for a fixed SF of 32 when there is no frequency offset since the frequency diversity allows the system to achieve higher absolute performance. However, as the frequency offset increases, higher SF_{time} gives better performance as the effect of the intercarrier interference becomes dominant. From Fig. 5, we can also see that, when the frequency offset is higher than 10% (normalized frequency offset=0.1), the BER performance starts to deteriorate, compared to the case of no offset, for the higher $\text{SF}_{freq}(\text{SF} = 2 \times 16)$. However, for lower $\text{SF}_{freq}(\text{SF} = 16 \times 2)$, the BER performance starts to degrade when the carrier frequency offset exceeds 20% of the frequency spacing between adjacent subcarriers. These results suggest that for a fixed total spreading factor, increasing SF_{time} with respect to SF_{freq} will decrease the sensitivity of the VSF-OFCDM system to the effect of the frequency offset. Therefore, increasing SF_{time} with respect to SF_{freq} for a total fixed SF of 32 will result in an overall better performance of the OFCDM system in the presence of considerable frequency offset.

Figures 6 and 7 show the BER of the MRC receiver versus E_b/N_o with 128 subcarriers having carrier frequency offsets of 0 and 30% for different number of users with total SF of 2×16 and 16×2, respectively. It can be observed from these figures that as the number of users increases, the degradation in performance increases as well for both spreading factors. This is to be expected since the intercarrier interference terms ICI_2 and ICI_g are proportional to the number of users. From Fig. 6, we can see that, for $\text{SF} = 2 \times 16$, the effect of increasing the frequency offset from 0 to 30% for 16 users is almost similar to doubling the number of users from 16 users to 32 users in terms of the degradation of the BER performance. From Fig. 6, we can see that, as the number of users increases from 16 to 32 users, the degradation of the BER performance due to the increase of frequency offset from 0 to 30% increases from approximately 0.29×10^{-2} to 3.7×10^{-2}. In Fig. 7, for $\text{SF} = 16 \times 2$, as the number of users

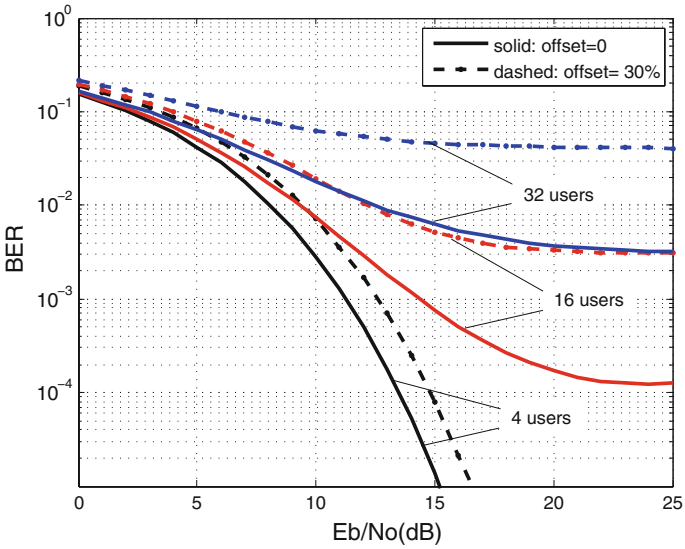

Fig. 6 BER of MRC receiver versus E_b/N_o with 128 subcarriers and SF $= 2 \times 16$ for different number of users at frequency offsets of 0 and 30%

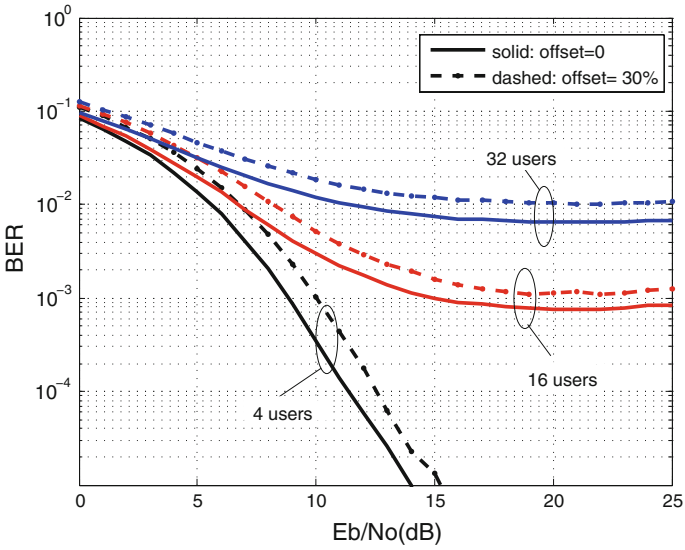

Fig. 7 BER of MRC receiver versus E_b/N_o with 128 subcarriers and SF $= 16 \times 2$ for different number of users at frequency offsets of 0 and 30%

increases from 16 to 32 users, the degradation of the BER performance due to the increase of frequency offset from 0 to 30% increases from approximately 0.5×10^{-3} to 3×10^{-3}. From these results, we can see that, the degradation due to increasing the number of users is more pronounced with the higher SF_{freq} since we have more subcarriers in each group.

4 CFO Estimation and Correction

Due to the adverse impact of frequency offset on VSF-OFCDM systems as seen in the previous section, a reliable estimation of the frequency offset is considered as a basic step in the coherent demodulation process. The carrier frequency offset estimation process can be divided into two fundamental steps which are coarse acquisition and tracking. In this work, we focus on the estimation and correction of the frequency offset in a tracking mode and a CFO correction scheme based on the maximum likelihood (ML) estimation principle is proposed. ML is chosen in our analysis as it is known to provide a consistent approach to parameter estimation problems and becomes minimum variance unbiased with the increase in the sample size [19].

4.1 Likelihood Function for Estimation

The log likelihood function considered in our analysis is given by [20]:

$$\Lambda = \frac{2}{N_o} \int_{T_o} \mathrm{Re}\left\{ r(t)\widetilde{r}^*(t) \right\} dt, \tag{23}$$

where T_o is the observation period and it should satisfy $T_o \geq T_c$.

We can write the received signal in (7) as

$$r(t) = \sum_{j} \sum_{g=1}^{G} \sum_{k=1}^{K_g} b_{j,g}^{(k)} \sum_{l=1}^{M} \alpha_{l,g} c_{j,l}^{F(k)} e^{i\left(2\pi(f_{l,g}+f_d)t+\phi_{l,g}\right)} \sum_{n=1}^{N} c_{j,l,n}^{T(k)} p(t-(jN+n)T_c) + n(t), \tag{24}$$

where $\widetilde{r}(t)$ is the estimate of $r(t)$ and is given by

$$\widetilde{r}(t) = \sum_{j} \sum_{g=1}^{G} \sum_{k=1}^{K_g} b_{j,g}^{(k)} \sum_{l=1}^{M} \alpha_{l,g} c_{j,l}^{F(k)} e^{i\left(2\pi(f_{l,g}+\widetilde{f}_d)t+\phi_{l,g}\right)} \sum_{n=1}^{N} c_{j,l,n}^{T(k)} p(t-(jN+n)T_c), \tag{25}$$

with $\widetilde{f}_d$ being estimate of the offset frequency f_d. A perfect estimation of the fading amplitude and phase is considered for each subcarrier.

Our objective is to maximize this likelihood function based on the ML estimation principle. We will assume in our analysis that the receiver performs the coarse frequency offset correction with training sequences before data transmission and we will consider the frequency offset in the tracking process only.

The log likelihood function depends on the data sequence and the number of subcarriers. The data dependence can be removed by averaging the log likelihood function over all the possible values of the data and fading parameters. In our case, we will define the dependence on data and fading parameters during the nth chip of the jth bit as follows:

$$d_{m,g} = \sum_{k=1}^{K_g} \alpha_{m,g} b_{j,g}^{(k)} c_{j,m}^{F(k)} c_{j,m,n}^{T(k)}. \tag{26}$$

The received signal can now be written as

$$r(t) = \sum_{g=1}^{G} \sum_{l=1}^{M} d_{l,g} e^{i\left(2\pi(f_{l,g}+f_d)t+\phi_{l,g}\right)} + n(t). \tag{27}$$

Considering the observation period to be T_c, the log likelihood function becomes

$$\Lambda = \frac{2}{N_o}\int_0^{T_c} \mathrm{Re}\left\{\sum_{g=1}^{G}\sum_{m=1}^{M} d_{m,g} r(t) e^{-i(2\pi f_{m,g}t+\phi_{m,g})} e^{-i(2\pi \widetilde{f}_d t)}\right\} dt$$
$$= \frac{2}{N_o}\sum_{g=1}^{G}\sum_{m=1}^{M} d_{m,g} \times \mathrm{Re}\{q_{m,g}\}, \tag{28}$$

where

$$q_{m,g} = \int_0^{T_c} r(t) e^{-i(2\pi f_{m,g}t+\phi_{m,g})} e^{-i(2\pi \widetilde{f}_d)t} dt,$$

which can be re-written as

$$q_{m,g} = \sum_{\acute{g}=1}^{G}\sum_{l=1}^{M}\int_0^{T_c} d_{l,\acute{g}} e^{i\left(2\pi(f_{l,\acute{g}}-f_{m,g}+\Delta f_d)t+\phi_{l,\acute{g}}-\phi_{m,g}\right)} dt,$$

where

$$\Delta f_d = f_d - \widetilde{f}_d.$$

Therefore, we can write $\mathrm{Re}\{q_{m,g}\}$ as in (29)

$$\mathrm{Re}\{q_{m,g}\} = \sum_{\acute{g}=1}^{G}\sum_{l=1}^{M}\int_0^{T_c} d_{l,\acute{g}} \cos\left(2\pi(f_{l,\acute{g}} - f_{m,g} + \Delta f_d)t + \phi_{l,\acute{g}} - \phi_{m,g}\right) dt \tag{29}$$
$$= \sum_{\acute{g}=1}^{G}\sum_{l=1}^{M} d_{l,\acute{g}} \frac{\sin(2\pi(f_{l,\acute{g}} - f_{m,g} + \Delta f_d)T_c + \phi_{l,\acute{g}} - \phi_{m,g}) - \sin(\phi_{l,\acute{g}} - \phi_{m,g})}{2\pi(f_{l,\acute{g}} - f_{m,g} + \Delta f_d)}.$$

The likelihood function is obtained as:

$$\bar{\Lambda} = e^{\Lambda} \tag{30}$$

In the case of low SINR, we can use the power series to expand the exponential. Therefore, the likelihood function for the carrier frequency offset is given by [21]:

$$\bar{\Lambda} = \frac{1}{N_o^2}\left(\sum_{g=1}^{G}\sum_{m=1}^{M} d_{m,g} \times \mathrm{Re}\{q_{m,g}\}\right)^2. \tag{31}$$

We remove the data dependence by averaging the likelihood function over all the values of the data and fading parameters $d_{m,g}$. After some calculations, we get

$$E[\bar{\Lambda}] = \frac{{T_c}^2 E[{d_{l,\acute{g}}}^2]}{4\pi^2 N_o^2}\sum_{g=1}^{G}\sum_{m=1}^{M}\sum_{\acute{g}=1}^{G}\sum_{l=1}^{M}\frac{1-\cos(2\pi\Delta f_d T_c)}{\left(\left(\Delta f_d + f_{l,\acute{g}} - f_{m,g}\right)T_c\right)^2},$$

where $\Delta f_d T_c$ is the normalized frequency offset error with respect to the subcarrier spacing.Figure 8 shows the normalized mean value of the likelihood function versus the normalized frequency offset error ($\Delta f_d T_c$) with 128 subcarriers. It can be seen from the figure that

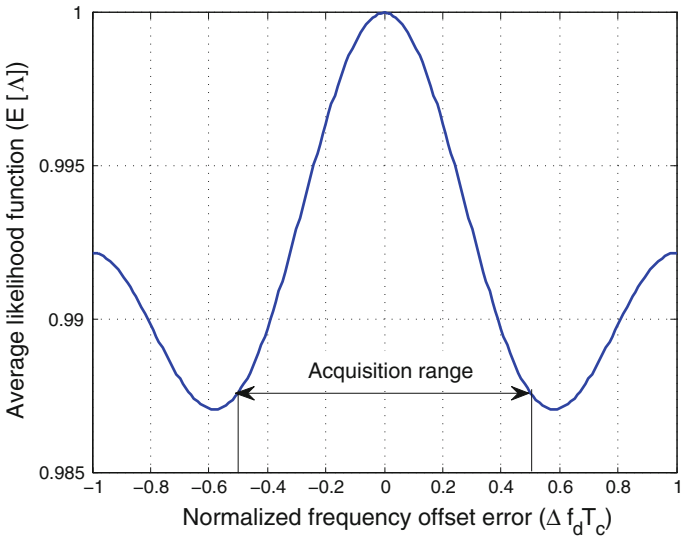

Fig. 8 Average value of the likelihood function versus the normalized frequency offset error

the likelihood function reaches a maximum value for $\Delta f_d T_c = 0$ and that the acquisition range is between -0.5 and 0.5 of the subcarrier spacing. The optimum value of $\widetilde{f}_d$ is therefore the one that maximizes the likelihood function. To find the maximum of this function, a non linear algorithm is employed as discussed in the next section.

4.2 Correction of CFO

Due to the characteristic of the likelihood function (local convexity of the function with respect to the normalized frequency offset error), we propose to use the gradient method to maximize the likelihood function. The gradient method is chosen because it is easy to implement and it requires low computational complexity [22].

Averaging on data and fading parameters and then taking the derivative of the likelihood function in (31) with respect to $\widetilde{f}_d$ to obtain the ML estimation, we get

$$\begin{aligned}\frac{\partial \bar{\Lambda}}{\partial \widetilde{f}_d} &= \frac{2C}{N_o^2}\sum_{g=1}^{G}\sum_{m=1}^{M}\mathrm{Re}\{q_{m,g}\}\frac{\partial \mathrm{Re}\{q_{m,g}\}}{\partial \widetilde{f}_d} \\ &= \frac{2C}{N_o^2}\sum_{g=1}^{G}\sum_{m=1}^{M}\mathrm{Re}\{q_{m,g}\}\times p_{m,g}, \end{aligned} \tag{32}$$

where

$$p_{m,g} = \frac{\partial \mathrm{Re}\{q_{m,g}\}}{\partial \widetilde{f}_d}.$$

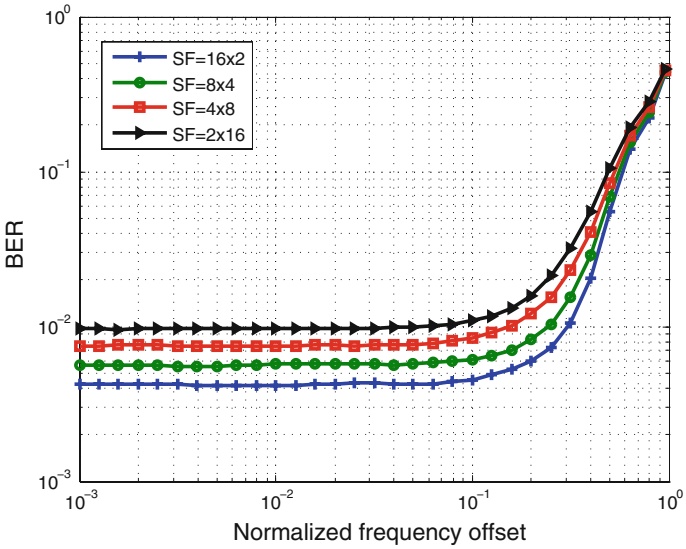

Fig. 9 BER versus normalized frequency offset at $E_b/N_o = 10$ dB for different SF

By differentiating (29), we get

$$p_{m,g} = 2\pi \sum_{\acute{g}=1}^{G} \sum_{l=1}^{M} \left[d_{l,\acute{g}} \int_0^{T_c} t \sin\left(2\pi(f_{l,\acute{g}} - f_{m,g} + \Delta f_d)t + \phi_{l,\acute{g}} - \phi_{m,g}\right) dt \right], \tag{33}$$

$$p_{m,g} = 2\pi \sum_{\acute{g}=1}^{G} \sum_{l=1}^{M} d_{l,\acute{g}} \left[\frac{[-T_c \cos(2\pi \Delta f_d T_c + \phi_{l,\acute{g}} - \phi_{m,g})]}{2\pi(f_{l,\acute{g}} - f_{m,g} + \Delta f_d)} + \frac{[\sin(2\pi \Delta f_d T_c + \phi_{l,\acute{g}} - \phi_{m,g}) - \sin(\phi_{l,\acute{g}} - \phi_{m,g})]}{(2\pi(f_{l,\acute{g}} - f_{m,g} + \Delta f_d))^2} \right]. \tag{34}$$

For the estimation of the frequency offset, we use the gradient method and hence,

$$\widetilde{f}_{d_{r+1}} = \widetilde{f}_{d_r} + k\epsilon_r,$$

where k is a positive constant, $\widetilde{f}_{d_r}$ and $\widetilde{f}_{d_{r+1}}$ are the estimation of f_d at the rth and $(r+1)$th iteration, respectively and ϵ_r is given by the following expression:

$$\epsilon_r = \sum_{g=1}^{G} \sum_{m=1}^{M} \mathrm{Re}\{q_{m,g}\} \times p_{m,g}. \tag{35}$$

4.3 Numerical Results

In this section, we use the same simulation parameters as in Sect. 3.2. Since we are interested in the low SINR region, we represent the results when using MRC receiver since it outperforms the EGC receiver in this region. Figure 9 shows the BER of the VSF-OFCDM system

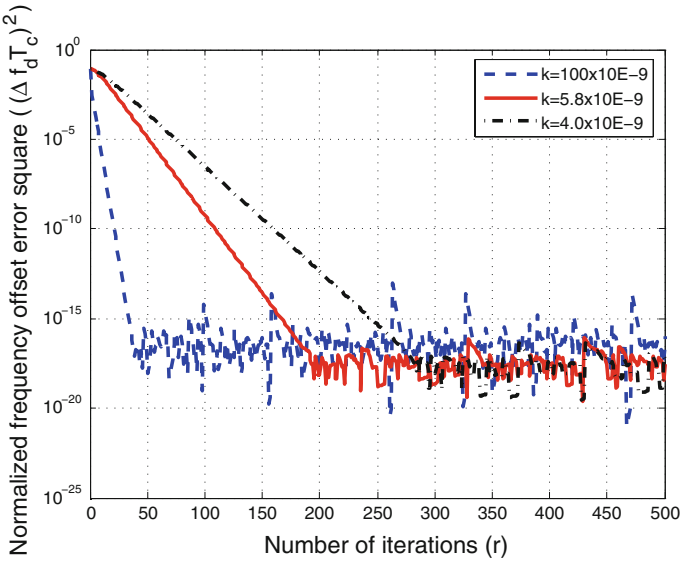

Fig. 10 CFO correction results versus number of iterations for different values of k and SF $= 2 \times 16$

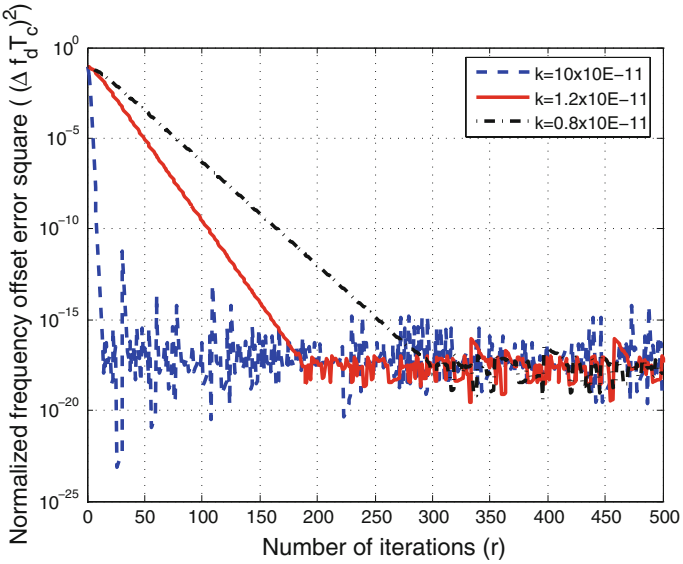

Fig. 11 CFO correction results versus number of iterations for different values of k and SF $= 16 \times 2$

versus the normalized (with respect to the subcarrier spacing) frequency offset ($f_d T_c$) for different spreading factors (SF $=$ SF$_{time} \times$ SF$_{freq}$) at $E_b/N_o = 10$ dB. This figure shows that for example, for a BER of 10^{-2}, the performance starts to deteriorate at $f_d T_c = 0.1, 0.2, 0.25$ and 0.3 for a total SF of 2×16, 4×8, 8×4 and 16×2, respectively. This means that if we can mitigate the frequency offset to less than that level for the different SF$_{time}$ and SF$_{freq}$, we can improve the system performance significantly.

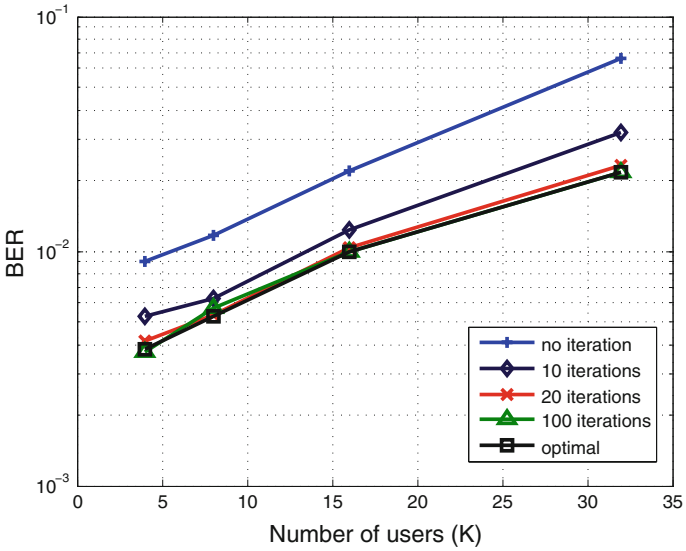

Fig. 12 BER performance improvement with different number of iterations and SF $= 2 \times 16$

We first investigate the convergence speed and the sensitivity of the gradient method with different spreading factors with 16 users simultaneously using the channel. In Figs. 10 and 11, the number of iterations are plotted versus the square of the normalized frequency offset error. In Fig. 10, we use a total SF of 2×16 which represents a case with high frequency domain spreading and we change the constant k to be $k = 100 \times 10^{-9}, k = 5.8 \times 10^{-9}$ and $k = 4 \times 10^{-9}$. The same is done in Fig. 11 but with a total SF of 16×2 and the constant k takes the values $k = 10 \times 10^{-11}, k = 1.2 \times 10^{-11}$ and $k = 0.8 \times 10^{-11}$. From Figs. 10 and 11, we notice that with different values of the constant k, the algorithm converges to the same floor of the normalized frequency offset error ($\Delta f_d T_c$) which is around 10^{-8} but at different convergence speeds. Also, different constants will result in different error variances after reaching the error floor. This is because different values of k result in different step sizes of converging to the optimal value (when there is no frequency offset) which affects the rapidity of convergence. If the constant is too large, the algorithm will fluctuate the frequency around the correct value. Smaller values of k will result in smaller error variance but the algorithm will require more iterations to converge to the optimal value. Similar figures can be obtained for the different spreading factors for different values of k. From Figs. 10 and 11, it is clear that different SF in the time and frequency domain will require different step sizes to converge at the same speed.

Figures 12 and 13 show the BER vs. the number of users with 128 subcarriers and initial normalized frequency offset (with respect to the subcarrier spacing) of 0.3 for different number of iterations with total SF of 2×16 and 16×2, respectively. The BER is calculated using Eqs. (9)–(22) together with the results of the normalized frequency offset error after a fixed number of iterations obtained from Figs. 10 and 11, for a total SF of 2×16 and 16×2, respectively. The value of the constant k is appropriately adjusted such that after the same number of iterations, the frequency offsets converge to the same value in all the cases. It was shown in Sect. 3.2 that, when the total spreading factor is fixed to 32, the OFCDM system with higher SF_{freq} is more sensitive to frequency offset than that with lower SF_{freq}. This effect can be seen in Figs. 12 and 13, where lower SF_{freq} converges faster to

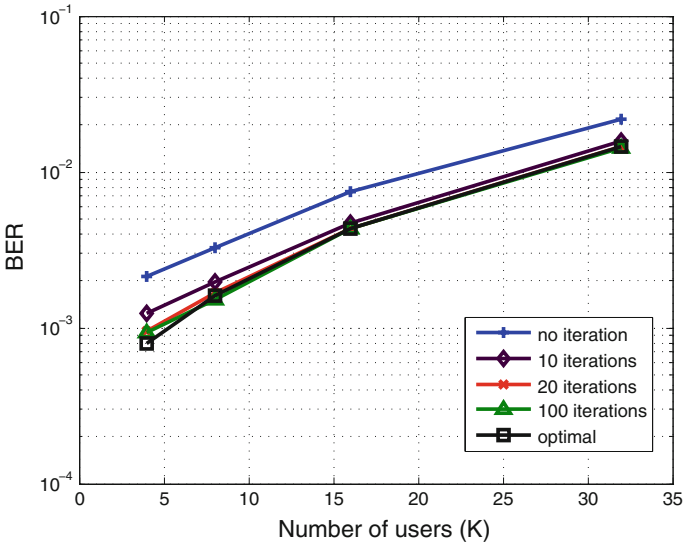

Fig. 13 BER performance improvement with different number of iterations and SF $= 16 \times 2$

the optimal value. The figures show that within only 20 iterations, we are close to the optimal value when the normalized frequency offset can be minimized to the case with negligible offset, which significantly improves the BER performance for different number of users and different spreading factors.

5 Conclusions

VSF-OFCDM systems can achieve the high capacity and high data rates that are expected from the 4G systems. They, like other multicarrier systems, suffer from performance degradation due to carrier frequency offset. In this article, the BER performance of downlink VSF-OFCDM was analyzed in the presence of carrier frequency offset for both MRC and EGC receivers. From the numerical results, we conclude that, when the total spreading factor is fixed, the VSF-OFCDM system with higher SF_{freq} is more sensitive to frequency offset than that with lower SF_{freq}. Also, the effect of the normalized frequency offset on BER performance is smaller when the normalized frequency offset is less than 10% for the higher SF_{freq} and less than 20% for the lower SF_{freq}. In addition, our results show that the degree of degradation due to CFO in the VSF-OFCDM system is also a function of the number of users. We showed that the BER performance of VSF-OFCDM can be improved significantly when the effect of frequency offset is mitigated. We presented a ML estimation of the CFO in a VSF-OFCDM system for the case of low SINR. The results show that the likelihood function reaches a maximum value when the normalized frequency offset is zero. Using the characteristics of the likelihood function and the ML principle, a gradient algorithm was used to minimize the frequency offset for different spreading factors. The numerical results show that our approach is able to estimate and correct the frequency offset with a normalized residual error of less than 10^{-8} for different spreading factors. Different spreading factors in time and frequency domain require different step sizes to converge at the same speed. The results also show that the BER of the VSF-OFCDM system can be improved significantly for different spreading factors after only a few number of iterations.

Appendix

In this appendix, we derive each of the terms in (8). The desired signal term, S, can be written as:

$$S = \frac{1}{T_c}\sqrt{\frac{P}{2}} b_{j,1}^{(1)} \sum_{m=1}^{M} \left(\alpha_{m,1}^{(1)}\right)^2 \left[c_{j,m}^{F(1)} c_{j,m}^{F(1)}\right] \times \sum_{n=1}^{N} \int_{(jN+n)T_c}^{(jN+n+1)T_c} \left[c_{j,m,n}^{T(1)} c_{j,m,n}^{T(1)}\right] p(t-(jN+n)T_c) \cos\left(\omega_d^{(1)} t + \phi_{m,1}^{(1)} - \hat{\phi}_{m,1}^{(1)}\right) dt. \tag{36}$$

where $c_{j,m,n}^{T(1)}$ is the nth chip in the time domain spreading code of user 1 on the mth subcarrier during the jth transmitted symbol and $c_{j,m}^{F(1)}$ is the mth chip in the frequency domain spreading sequence of user 1 during the jth transmitted symbol. The rectangular function, $p(t-(jN+n)T_c)$, has a constant amplitude of unity over T_c and since $b_{j,1}^{(1)}$, $[c_{j,m}^{F(1)} c_{j,m}^{F(1)}]$ and $(\alpha_{j,m}^{(1)})^2$ are constants over T_c, they can be taken outside the integral. In addition, since the system spreading codes are synchronized at the receiver, $[c_{j,m}^{F(1)} c_{j,m}^{F(1)}] = 1$ and $[c_{j,m,n}^{T(1)} c_{j,m,n}^{T(1)}] = 1$. Therefore, the desired signal term can be written as:

$$S = \sqrt{\frac{P}{2}} b_{j,1}^{(1)} \frac{\sin\left(\frac{\omega_d^{(1)} T_c}{2}\right)}{\left(\frac{\omega_d^{(1)} T_c}{2}\right)} \sum_{m=1}^{M} \left(\alpha_{m,1}^{(1)}\right)^2 \sum_{n=1}^{N} \cos\left((jN+n+1/2)\omega_d^{(1)} T_c + \phi_{m,1}^{(1)} - \hat{\phi}_{m,1}^{(1)}\right), \tag{37}$$

The noise term, η, can be expressed as follows:

$$\eta = \frac{1}{T_c} \sum_{m=1}^{M} \alpha_{m,1}^{(1)} c_{j,m}^{F(1)} \sum_{n=1}^{N} c_{j,m,n}^{T(1)} \int_{(jN+n)T_c}^{(jN+n+1)T_c} p(t-(jN+n)T_c) n(t) \cos\left(\omega_{m,1} t + \hat{\phi}_{m,1}^{(1)}\right) dt. \tag{38}$$

The noise term η is a Gaussian random variable with zero mean and its variance is given by:

$$\sigma_\eta^2 = E[\eta^2] = \frac{N N_0}{4 T_c} \sum_{m=1}^{M} \left(\alpha_{m,1}^{(1)}\right)^2. \tag{39}$$

The interference term MAI is obtained from (5) with the condition that $g = 1$ and $l = m$ for $k \neq 1$. Therefore,

$$\text{MAI} = \frac{1}{T_c}\sqrt{\frac{P}{2}} \sum_{k=2}^{K_1} b_{j,1}^{(k)} \sum_{m=1}^{M} \alpha_{m,1}^{(1)} \alpha_{m,1}^{(k)} c_{j,m}^{F(1)} c_{j,m}^{F(k)} \times \sum_{n=1}^{N} \int_{(jN+n)T_c}^{(jN+n+1)T_c} c_{j,m,n}^{T(1)} c_{j,m,n}^{T(k)} p(t-(jN+n)T_c) \cos\left(\omega_d^{(k)} t + \phi_{m,1}^{(k)} - \hat{\phi}_{m,1}^{(1)}\right) dt, \tag{40}$$

where K_1 is the total number of users in group 1. We can express the MAI term as follows:

$$\text{MAI} = \sqrt{\frac{P}{2}} \sum_{k=2}^{K_1} \sum_{m=1}^{M} \sum_{n=1}^{N} b_{j,1}^{(k)} \frac{\sin\left(\frac{\omega_d^{(k)} T_c}{2}\right)}{\left(\frac{\omega_d^{(k)} T_c}{2}\right)} \alpha_{m,1}^{(1)} \alpha_{m,1}^{(k)} c_{j,m}^{F(1)} c_{j,m}^{F(k)} \times c_{j,m,n}^{T(1)} c_{j,m,n}^{T(k)} \cos\left((jN + n + 1/2)\omega_d^{(k)} T_c + \phi_{m,1}^{(k)} - \hat{\phi}_{m,1}^{(1)}\right). \tag{41}$$

The MAI is approximated by a Gaussian random variable with zero mean and its variance is given by:

$$\sigma_{\text{MAI}}^2 = N \frac{P}{4} (K_1 - 1) E\left[\left(\alpha_{m,1}^{(k)}\right)^2 \frac{\sin^2\left(\frac{\omega_d^{(k)} T_c}{2}\right)}{\left(\frac{\omega_d^{(k)} T_c}{2}\right)^2} \right] \sum_{m=1}^{M} \left(\alpha_{m,1}^{(1)}\right)^2, \tag{42}$$

where $\phi_{m,1}^{(k)}$ and $\hat{\phi}_{m,1}^{(1)}$ are i.i.d. random variables uniformly distributed over the interval $[0, 2\pi)$. The term $[(jN + n + 1/2)\omega_d^{(k)} T_c]$ only rotates the phase $[\phi_{m,1}^{(k)} - \hat{\phi}_{m,1}^{(1)}]$. Therefore, $E[\cos^2((jN + n + 1/2)\omega_d^{(k)} T_c + \phi_{m,1}^{(k)} - \hat{\phi}_{m,1}^{(1)})]$ is equal to 0.5.

The self-intercarrier interference term ICI_1 can be obtained from (5) by letting $k = 1$, $g = 1$ and $l \neq m$. Therefore,

$$\text{ICI}_1 = \frac{1}{T_c} \sqrt{\frac{P}{2}} b_{j,1}^{(1)} \sum_{m=1}^{M} \sum_{\substack{l=1 \\ l \neq m}}^{M} \alpha_{m,1}^{(1)} \alpha_{l,1}^{(1)} c_{j,m}^{F(1)} c_{j,l}^{F(1)} \times \sum_{n=1}^{N} \int_{(jN+n)T_c}^{(jN+n+1)T_c} c_{j,m,n}^{T(1)} c_{j,l,n}^{T(1)} p(t - (jN + n)T_c) \times \cos\left(\left(\omega_d^{(1)} + \omega_{l,1} - \omega_{m,1}\right) t + \phi_{l,1}^{(1)} - \hat{\phi}_{m,1}^{(1)}\right) dt, \tag{43}$$

The expression for the term ICI_1 can be written as:

$$\text{ICI}_1 = \sqrt{\frac{P}{2}} b_{j,1}^{(1)} \sum_{m=1}^{M} \sum_{\substack{l=1 \\ l \neq m}}^{M} \sum_{n=1}^{N} \frac{\sin\left(\frac{\omega_d^{(1)} T_c}{2}\right)}{\left(\frac{(\omega_d^{(1)} + \omega_{l,1} - \omega_{m,1}) T_c}{2}\right)} \times \alpha_{m,1}^{(1)} \alpha_{l,1}^{(1)} c_{j,m}^{F(1)} c_{j,l}^{F(1)} c_{j,m,n}^{T(1)} c_{j,l,n}^{T(1)} \cos\left((jN + n + 1/2)(\omega_d^{(1)} + \omega_{l,1} - \omega_{m,1}) T_c + \phi_{l,1}^{(1)} - \hat{\phi}_{m,1}^{(1)}\right). \tag{44}$$

The ICI_1 can be approximated by a Gaussian random variable with zero mean and its variance is given by:

$$\sigma_{\text{ICI}_1}^2 = N \frac{P}{4} \sum_{m=1}^{M} \left(\alpha_{m,1}^{(1)}\right)^2 \sum_{\substack{l=1 \\ l \neq m}}^{M} \left(\alpha_{l,1}^{(1)}\right)^2 \frac{\sin^2\left(\frac{\omega_d^{(1)} T_c}{2}\right)}{\left(\frac{(\omega_d^{(1)} + \omega_{l,1} - \omega_{m,1}) T_c}{2}\right)^2}. \tag{45}$$

The multiple access interference from users in the same group as the desired user, but associated with the subcarriers different from the considered subcarrier, ICI_2, is obtained by setting $k \neq 1$, $g = 1$ and $l \neq m$ in (5). Therefore,

$$\begin{aligned}\mathrm{ICI}_2 = \frac{1}{T_c}\sqrt{\frac{P}{2}} \sum_{k=2}^{K_1} b_{j,1}^{(k)} \sum_{m=1}^{M} \sum_{\substack{l=1 \\ l\neq m}}^{M} \alpha_{m,1}^{(1)} \alpha_{l,1}^{(k)} c_{j,m}^{F(1)} c_{j,l}^{F(k)} \\ \times \sum_{n=1}^{N} \int_{(jN+n)T_c}^{(jN+n+1)T_c} c_{j,m,n}^{T(1)} c_{j,l,n}^{T(k)} p(t-(jN+n)T_c) \\ \times \cos\left(\left(\omega_d^{(k)} + \omega_{l,1} - \omega_{m,1}\right) t + \phi_{l,1}^{(k)} - \hat{\phi}_{m,1}^{(1)}\right) dt, \end{aligned} \tag{46}$$

We can express this term as:

$$\begin{aligned}\mathrm{ICI}_2 = \sqrt{\frac{P}{2}} \sum_{k=2}^{K_1} \sum_{m=1}^{M} \sum_{\substack{l=1 \\ l\neq m}}^{M} \sum_{n=1}^{N} b_{j,1}^{(k)} \frac{\sin\left(\frac{\omega_d^{(k)} T_c}{2}\right)}{\left(\frac{(\omega_d^{(k)} + \omega_{l,1} - \omega_{m,1}) T_c}{2}\right)} \\ \times \alpha_{m,1}^{(1)} \alpha_{l,1}^{(k)} c_{j,m}^{F(1)} c_{j,m,n}^{T(1)} c_{j,l}^{F(k)} c_{j,l,n}^{T(k)} \\ \times \cos\left((jN+n+1/2)(\omega_d^{(k)} + \omega_{l,1} - \omega_{m,1}) T_c + \phi_{l,1}^{(k)} - \hat{\phi}_{m,1}^{(1)}\right). \end{aligned} \tag{47}$$

The ICI_2 can be approximated by a Gaussian random variable with zero mean and variance given by:

$$\sigma_{\mathrm{ICI}_2}^2 = N(K_1 - 1)\frac{P}{4} \sum_{m=1}^{M} \left(\alpha_{m,1}^{(1)}\right)^2 E\left[\left(\alpha_{l,1}^{(k)}\right)^2 \frac{\sin^2\left(\frac{\omega_d^{(k)} T_c}{2}\right)}{\left(\frac{(\omega_d^{(k)} + \omega_{l,1} - \omega_{m,1}) T_c}{2}\right)^2}\right]. \tag{48}$$

The interference from other groups ICI_g can be obtained from (5) by letting $g \neq 1$. Therefore,

$$\begin{aligned}\mathrm{ICI}_g = \frac{1}{T_c}\sqrt{\frac{P}{2}} \sum_{g=2}^{G} \sum_{k=1}^{K_g} b_{j,g}^{(k)} \sum_{m=1}^{M} \sum_{l=1}^{M} \alpha_{m,1}^{(1)} \alpha_{l,g}^{(k)} c_{j,m}^{F(1)} c_{j,l}^{F(k)} \\ \times \sum_{n=1}^{N} \int_{(jN+n)T_c}^{(jN+n+1)T_c} c_{j,m,n}^{T(1)} c_{j,l,n}^{T(k)} p(t-(jN+n)T_c) \\ \times \cos\left(\left(\omega_d^{(k)} + \omega_{l,g} - \omega_{m,1}\right) t + \phi_{l,g}^{(k)} - \hat{\phi}_{m,1}^{(1)}\right) dt, \end{aligned} \tag{49}$$

This term can also be expressed as follows:

$$\begin{aligned}\mathrm{ICI}_g = \sqrt{\frac{P}{2}} \sum_{g=2}^{G} \sum_{k=1}^{K_g} \sum_{m=1}^{M} \sum_{l=1}^{M} \sum_{n=1}^{N} b_{j,g}^{(k)} \frac{\sin\left(\frac{\omega_d^{(k)} T_c}{2}\right)}{\left(\frac{\left(\omega_d^{(k)} + \omega_{l,g} - \omega_{m,1}\right) T_c}{2}\right)} \\ \times \alpha_{m,1}^{(1)} \alpha_{l,g}^{(k)} c_{j,m}^{F(1)} c_{j,m,n}^{T(1)} c_{j,l}^{F(k)} c_{j,l,n}^{T(k)} \\ \times \cos\left((jN + n + 1/2)\left(\omega_d^{(k)} + \omega_{l,g} - \omega_{m,1}\right) T_c + \phi_{l,g}^{(k)} - \hat{\phi}_{m,1}^{(1)}\right). \end{aligned} \tag{50}$$

The ICI_g can be approximated by a Gaussian random variable with zero mean and variance given by:

$$\sigma^2_{\mathrm{ICI}_g} = N \frac{P}{4} \sum_{g=2}^{G} K_g \sum_{m=1}^{M} \left(\alpha_{m,1}^{(1)}\right)^2 E\left[\left(\alpha_{l,g}^{(k)}\right)^2 \frac{\sin^2\left(\frac{\omega_d^{(k)} T_c}{2}\right)}{\left(\frac{\left(\omega_d^{(k)} + \omega_{l,g} - \omega_{m,1}\right) T_c}{2}\right)^2}\right]. \tag{51}$$

Using the assumption in [5] that the frequency offset is equal and constant for all users, therefore, $\omega_d^{(k)} = \omega_d$. Also, we can assume the estimated phase for user 1 in group 1 to be $\hat{\phi}_{m,1}^{(1)} = (jN + n + 1/2)\omega_d T_c + \phi_{m,1}^{(1)}$ [23]. This means that the subcarrier phase estimator determines the value of the phase rotation at time $(n + 1/2)T_c$ which is the middle of the nth chip integration interval. Since in our analysis, we consider downlink transmission; therefore, we can also assume that all the users suffer equal fading gain and phase shift on each subcarrier [6], which means that $\alpha_{m,g}^{(k)} = \alpha_{m,g}$. Using these assumptions, the terms in (9)-(13) and in (20) are obtained.

References

1. Xiao, L., & Liang, Q. (2000). A Novel MC-2D-CDMA communication system and its detection methods. *IEEE International Conference on Communications, 3*, 1223–1227.
2. Atarashi, H., Abeta, S., & Sawahashi, M. (2003). Variable spreading factor orthogonal frequency and code division multiplexing (VSF-OFCDM) for broadband packet wireless access. *IEICE Transactions on Communications, E86-B*, 291–299.
3. Maeda, N., Kishiyama, Y., Atarashi, H., & Sawashashi, M. (2003). Variable spreading factor-OFCDM with two dimensional spreading that prioritizes time domain spreading for forward link broadband wireless access. *IEEE Vehicular Technology Conference, 1*, 127–132.
4. Azmi, P., & Tavakkoli, N. (2008). Narrow-band interference suppression in CDMA spread-spectrum communication systems using preprocessing based techniques in transform-domain. *Progress in Electromagnetics Research Letters, 3*(1), 141–150.
5. Kim, Y., Choi, S., You, C., & Hong, D. (1999). Effect of carrier frequency offset on the performance of an MC-CDMA system and its countermeasure using pulse shaping. *IEEE International Conference on Communications, 1*, 167–171.
6. Yang, W., Liu, J., & Cheng, S.-X. (2006). Effect of carrier-frequency offset on the performance of group-orthogonal multicarrier CDMA systems. *Elsevier Signal Processing, 86*, 3934–3940.
7. Steendam, H., & Moeneclaey, M. (2001). The effect of carrier frequency offsets on downlink and uplink MC-DS-CDMA. *IEEE Journal on Selected Areas in Communications, 19*, 2528–2536.
8. Moon, J.-H., You, Y., Jeon, W.-G., & Paik, J.-H. (2004). BER performance of multiple-antenna OFCDM with imperfections. *IEEE Communications Letters, 8*, 12–14.
9. Nasser, Y., des Noes, M., Ros, L., & Jourdain, G. (2006). Sensitivity of OFDM-CDMA systems to carrier frequency offset. *IEEE International Conference on Communications, 10*, 4577–4582.

10. Chang, C., Huang, P., & Tu, T. (2007). Performance comparison of MRC and EGC on a MC-CDMA system with synchronization errors over fading channels. *Wireless Personal Communications, 43*, 685–698.
11. Pursley, M. (1977). Performance evaluation for phase coded spread spectrum multiple access communication-part I: System analysis. *IEEE Transactions on Communications, COM-25*, 795–799.
12. Daffara, F., & Chouly, A. (1993). Maximum likelihood frequency detectors for orthogonal multicarrier systems. *IEEE International Conference on Communications, 2*, 766–771.
13. Guainazzo, M., Gandetto, M., Sacchi, C., & Regazzoni, C. S. (2003). Maximum likelihood estimation of carrier offset in a variable bit rate orthogonal multicarrier CDMA. *IEEE International Symposium on Image and Signal Processing and Analysis, 2*, 1181–1185.
14. Maeda, N., Atarashi, H., & Sawahashi, M. (2003). Performance comparison of channel interleaving methods in frequency domain for VSF-OFCDM broadband wireless access in forward link. *IEICE Transactions on Communications, E86-B*, 300–313.
15. Caldwell, R., & Anpalagan, A. (2006). Performance analysis of subcarrier allocation in two dimensionally spread OFCDM systems. In *IEEE Vehicular Technology Conference*.
16. Weinstein, S. B., & Ebert, P. M. (1971). Data transmission by frequency division multiplexing using the discrete fourier transform. *IEEE Transactions on Communications, 19*, 628–634.
17. Jakes, C. J. (1994). *Microwave mobile communications*. New Jersy: IEEE Press.
18. Long, H., & Chew, Y. H. (2004). An adaptive subcarrier allocation scheme for MC-DS-CDMA systems in the presence of multiple access interference. *IEEE International Conference on Communications, 5*, 2894–2898.
19. Isaac, O., Zhang, Y., & Shirisha, P. (2006). *OFDM carrier frequency offset estimation*. Ph.D thesis, Karlstad University, Sweden.
20. Proakis, J. G. (2001). *Digital communications* (4th ed.). New York: McGraw Hill.
21. Q. Tian, Letaief, K. B. (2001). ML estimation and correction of frequency offset for MC-CDMA systems over fading channels. *IEEE Vehicular Technology Conference, 1*, 571–575.
22. Kelley, C. T. (1999). *Iterative methods for optimization*. Philadelphia, PA: Society of Industrial and Applied Mathematics (SIAM).
23. Shi, Q., & Latva-aho, M. (2001). Effect of frequency offset on the performance of asynchronous MC-CDMA systems in a correlated Rayleigh fading channel. *IEEE International Conference on Info-Tech and Info-Net, 2*, 448–452.

Author Biographies

Lamiaa Khalid is a Ph.D. candidate in Radio Resource Management (RRM) Research Group of the WINCORE Lab at Ryerson University. She received her B.Sc. degree in Electrical Engineering from Ain Shams University, Egypt in 2000. From 2000 to 2005, she was working as a full-time teacher assistant in the Department of Electrical Engineering in October 6 University, Egypt. In September 2005, she joined RRM Research Group as a research assistant and completed her M.A.Sc. degree in December 2007. Her Research interests are wireless and mobile communications and radio resource management, particularly adaptive modulation and coding and power adaptation in multi-user communication systems and cognitive radio systems.

Alagan Anpalagan received B.A.Sc., M.A.Sc., and Ph.D. degrees in Electrical Engineering from the University of Toronto, Canada in 1995, 1997 and 2001 respectively. Since 2001, he has been with the Ryerson University, Toronto, Canada, where he co-founded WINCORE laboratory and leads a research group working on two areas: radio resource management (RRM) and radio access & networking (RAN). Currently, he is an Associate Professor and Program Director for Electrical Engineering.

His research interests are in general: wireless communication, mobile networks and system performance analysis; and in particular, multicarrier spread spectrum systems, cooperative, cognitive and multihop communications, radio resource management, and cross-layer resource optimization. He has published more than 100 papers in international journals and conference proceedings. Prior to his academic career, he was a Technical Consultant at Bell Mobility working on 1xRTT system deployment studies in 2001 and in 1997 he was with Nortel Networks working on R&D projects in systems engineering.

Dr. Anpalagan served as Technical Program Co-Chair, IEEE Canadian Conference on Electrical and Computer Engineering (2004, 2008) and Chair, IEEE Toronto Section (2006–2007), Chair, Communications Chapter (2004–2005), Editor—EURASIP Journal of Wireless Communications and Networking, Guest Editor for two special issues on Radio Resource Management for 3G+ Wireless Systems and Fairness in Radio Resource Management for Wireless Networks in EURASIP. Currently, he serves as Editor, Wireless Personal Communication. Dr. Anpalagan currently serves as Chair, IEEE Toronto Appointments and Nominations Committee, Chair of Professional Development Committee, IEEE Canada and Member of IEEE Globalization of Professional Activities Committee. He is the recipient of an IEEE Canada Award in 2005 for his technical leadership. He is an IEEE Senior Member and a Registered Professional Engineer in the province of Ontario, Canada.